



Short communication

Partial oxidation of methane in a $Zr_{0.84}Y_{0.16}O_{1.92}-La_{0.8}Sr_{0.2}Cr_{0.5}Fe_{0.5}O_{3-\delta}$ hollow fiber membrane reactor targeting solid oxide fuel cell applications

Jian-jun Liu, Shang-quan Zhang, Wen-dong Wang, Jian-feng Gao, Wei Liu, Chu-sheng Chen*

Laboratory of Materials for Energy Conversion, Department of Materials Science and Engineering, University of Science and Technology of China, Hefei, Anhui 230026, PR China

HIGHLIGHTS

- A hollow fiber membrane reactor can convert methane into H_2 and CO efficiently.
- SOFC can run on the fuel converted from methane by the membrane reactor.
- The membrane reactor is promising for methane fuel processing application in SOFCs.

ARTICLE INFO

Article history:

Received 13 April 2012

Received in revised form

8 June 2012

Accepted 9 June 2012

Available online 16 June 2012

Keywords:

Partial oxidation of methane
Methane reforming
Membrane reactor
Solid oxide fuel cell

ABSTRACT

A membrane reactor has been investigated to reform methane into fuel suitable for solid oxide fuel cells (SOFCs). An oxygen-permeable $Zr_{0.84}Y_{0.16}O_{1.92}$ (YSZ)– $La_{0.8}Sr_{0.2}Cr_{0.5}Fe_{0.5}O_{3-\delta}$ (LSCF) hollow fiber membrane coated with Ru catalyst at the lumen side is used to construct the reactor. The reactor is tested at elevated temperatures with the shell and lumen sides of the hollow fiber exposed to the atmosphere air and methane, respectively. The reaction of methane with the permeated oxygen proceeds at a remarkably fast rate. Methane throughput conversion over 90% is attained at 950 °C at a high methane feed rate of $14.7 \text{ cm}^3 \text{ CH}_4 \text{ min}^{-1} \text{ cm}^{-2}$ membrane surface and oxygen permeation rate $7.9 \text{ cm}^3 \text{ min}^{-1} \text{ cm}^{-2}$; the effluent from the reactor is composed mainly of H_2 (53.5%) and CO (35.7%), revealing that the dominating reaction occurring in the reactor is partial oxidation of the methane (POM). When the effluent is fed into a disk-shaped SOFC single cell, it exhibits stable performance. The mild exothermal nature of POM reaction and the high surface to volume ratio of hollow fiber membrane may allow us to construct and operate a compact autothermal methane reformer for SOFC applications.

© 2012 Elsevier B.V. All rights reserved.

1. Introduction

Solid oxide fuel cell (SOFC) is an emerging clean and efficient power production technology. It is best operated with hydrogen as fuel in terms of anode activity [1–6]. The use of hydrogen fuel is however limited by the lack of infrastructure for production, distribution and storage. Therefore, it has been proposed to directly use methane [2–5] and other hydrocarbon [6,7] as fuel for SOFC. The primary problem in using carbonaceous fuels is the deposition of carbon on the Ni-based anode of SOFC [4–6]. One way to solve avoid this problem is to use carbon-resistant anodes [8–10]. Although progresses have been made in developing carbon-resistant anodes, the state-of-art anode for SOFC remains Ni in composite with electrolyte. The thermodynamic calculation has

indicated that the carbonaceous fuel will not undertake carbon deposition with proper C–H–O ratio [11,12]. The desired ratio can be attained by reforming of carbonaceous fuel.

Steam reforming (SR) is the main route for reforming of methane for SOFC application. One can conduct SR inside the SOFC stack for the sake of system compactness [13–17]. Since most of the methane is reacted at the injection port of SOFC, resulting in a local cooling due to the highly endothermic nature of SR reaction. Consequently, local thermal stress is introduced, resulting in the failure of the SOFC stack [17,18]. Alternatively, one can perform SR outside the SOFC stack. Due to the highly endothermic nature of the SR reaction, a large quantity of heat needs to be fed into the reactor. Consequently, it is not feasible economically to operate a SR reactor at a size required by SOFC [19–21].

Partial oxidation of methane (POM) may also be used for processing of methane for SOFC. Unlike SR, POM is mild exothermal reaction, thus it may operate without external heating. The main difficulty with POM lies in the consumption of pure oxygen that is

* Corresponding author. Tel.: +86 551 3602940; fax: +86 551 3631760.

E-mail address: ccsm@ustc.edu.cn (C.-s. Chen).

currently produced by cryogenic air separation process. This difficulty may be overcome by making use of oxygen-permeable dense ceramic membrane. The dense membrane is made of mixed oxygen ionic and electronic conductor, allowing oxygen to permeate through while being impermeable to nitrogen and other gaseous species. An important application of the membrane is to integrate the POM reaction with separation of oxygen in a single space (Fig. 1) [22–27]. For this reactor application, the membrane must exhibit both high oxygen permeability and stability under stringent operation conditions with one side of the membrane exposed to oxidative atmosphere (air) and the other side highly reducing atmosphere containing CH_4 , H_2 and CO . It has been shown that the membrane made of the single-phase mixed conducting oxide, such as $\text{La}_{0.4}\text{Sr}_{0.6}\text{Co}_{0.2}\text{Fe}_{0.8}\text{O}_{3-\delta}$ [22] and $\text{Ba}_{0.5}\text{Sr}_{0.5}\text{Co}_{0.8}\text{Fe}_{0.2}\text{O}_{3-\delta}$ [23], possesses sufficiently high oxygen permeability, but its long-term stability is problematic under the POM reactor condition. Recently, we have found that the $\text{Zr}_{0.84}\text{Y}_{0.16}\text{O}_{1.92}$ – $\text{La}_{0.8}\text{Sr}_{0.2}\text{Cr}_{0.5}\text{Fe}_{0.5}\text{O}_{3-\delta}$ (YSZ–LSCF) dual-phase composite membrane in hollow fiber geometry can meet both the oxygen permeation and stability requirement under POM-relevant conditions [28]. Therefore, in the present work, a POM catalytic membrane reactor built with the YSZ–LSCF hollow fiber was investigated, and its applicability to the SOFC was examined by testing a disk-shaped SOFC cell using the methane processed with the hollow fiber POM reactor.

2. Experimental

The YSZ–LSCF hollow fiber was prepared using a combination of phase-inversion and sintering technique [28,29]. The starting suspension consisted of 43.85 wt% YSZ powders, 32.24 wt% LSCF powders, 19.59 wt% N-methyl-2-pyrrolidone (CP, Sinopharm Chemical Reagent Co.), 3.46 wt% polyethersulfone (Radel A-100, Solvay Advanced Polymers) and 0.09 wt% polyvinylpyrrolidone (K30, Sinopharm Chemical Reagent Co.). The suspension was stirred for 48 h and degassed for 2 h, then extruded through a tube-in-orifice spinneret (outer diameter 2.6 mm, inner diameter 1.2 mm) using a pressurized nitrogen (3 bar). The fiber emerging from the spinneret passed through an air gap (1 cm) and immersed in a water bath to complete solidification. The injection rate of internal water was 4 ml min^{-1} . After desiccation for 48 h, the fiber was sintered at 1430°C for 10 h in the air.

The lumen side of the sintered hollow fiber was coated with a Ru catalyst. RuCl_3 and LSCF powder were weighed according to Ru/LSCF weight ratio of 1:2, dispersed in ethanol and ball-milled for one day to obtain a homogeneous suspension. The suspension was injected into the LSCF–YSZ hollow fiber, followed by drying at room temperature. This process was repeated several times to obtain sufficiently high catalyst loading. The hollow fiber coated with the catalyst was heat-treated at 1000°C for 50 min in the air.

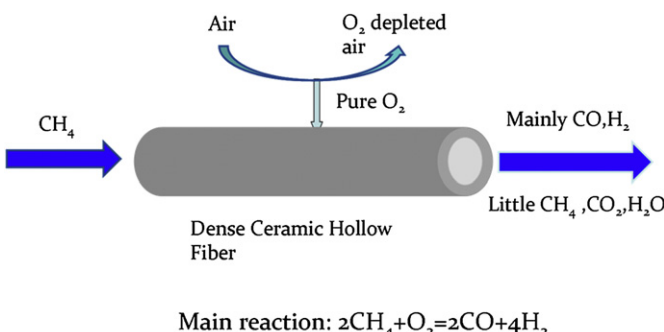


Fig. 1. Schematic of a membrane reactor for partial oxidation of methane.

The Ru loading was calculated from the loading mass of Ru/LSCF catalyst and the weight percentage of Ru in the catalyst. The morphology of the as-treated hollow fiber was examined by SEM (JSM-6390LA, JEOL, Japan).

A reactor was constructed by placing an YSZ–LSCF hollow fiber in between two coaxial alumina tubes and joining them with glass powder sealant; the schematic set-up of the reactor is similar to the one shown in Ref. [29]. The reactor was tested at elevated temperatures with the shell and lumen side exposed to the atmosphere air and methane, respectively. The effluent from the reactor was dried and analyzed by an online gas chromatography (GC) (1690, KeXiao, China and GC9750, FuLi, China). The GC was equipped with a thermal conductivity detector and two columns with one filled with 60–80 mesh GDX-502 for detection of CO_2 and another filled with 60–80 mesh 5A molecular sieves for detection of CO , CH_4 , O_2 and N_2 . The amount of H_2O contained in the effluent was determined with a hydrogen atomic balance.

A disk-shaped SOFC with $\text{NiO} + \text{YSZ}$ (40:60 vol) as anode, YSZ as electrolyte and $\text{La}_{0.8}\text{Sr}_{0.2}\text{MnO}_3 + \text{YSZ}$ (50:50 wt) as cathode was fabricated. The $\text{NiO} + \text{YSZ}/\text{YSZ}$ was prepared by dual-layer tape casting, and the cathode was prepared by screen printing. The electrolyte had a thickness of $20 \mu\text{m}$ and the effective cathode area is 0.237 cm^2 . Ag paste was used as current collector. The fuel converted from methane by the membrane reactor was feed into the SOFC as fuel, and its electrochemical performance was measured using an Electrochemical Workstation described elsewhere [30].

3. Results

The YSZ–LSCF hollow fiber used was 57.7 mm in length, 1.16 mm in inside diameter, and 0.34 mm in wall thickness. Fig. 2 gives the cross-section view of the hollow fiber membrane. A sponge-like porous catalyst layer was formed on the surface (at the lumen side). The thickness of the catalyst was estimated to be $\sim 5 \mu\text{m}$, Ru loading $\sim 7.6 \text{ mg cm}^{-2}$.

Fig. 3 shows the oxygen permeation rate as a function of temperature at a fixed methane feed rate of $20 \text{ cm}^3 \text{ min}^{-1}$. With temperature increased from 900 to 950°C , the oxygen permeation rate was raised from 5.5 to $8.1 \text{ cm}^3 \text{ min}^{-1} \text{ cm}^{-2}$; accordingly, the atomic O/C ratio in the effluent of the reactor changed from 1.16 to 1.71. Fig. 4 shows the oxygen permeation rate as a function of methane feed rate at a fixed temperature of 950°C . It can be seen that the oxygen permeation rate increased with increasing CH_4 feed

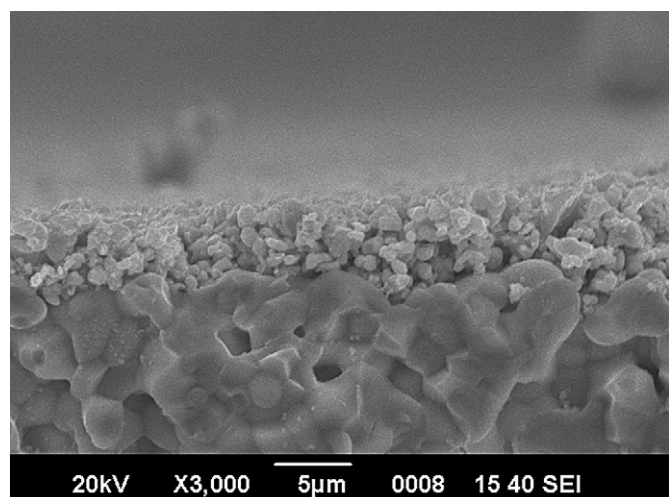


Fig. 2. SEM image of cross-section of the YSZ–LSCF hollow fiber membrane coated with Ru catalyst at the lumen side.

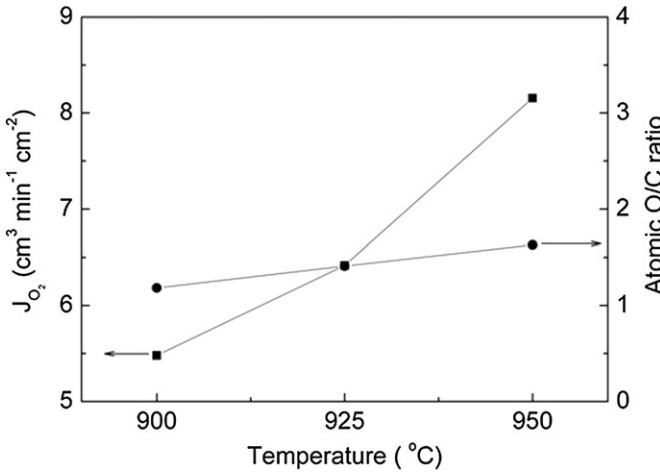


Fig. 3. Temperature dependence of (■) oxygen permeation rate and (●) atomic O/C ratio at a fixed CH_4 feed rate of $20 \text{ cm}^3 \text{ min}^{-1}$.

rate to $\sim 16 \text{ cm}^3 \text{ min}^{-1}$; after that it leveled off. The atomic O/C ratio in the effluent changed accordingly. At a lower methane feed rate of $7.5 \text{ cm}^3 \text{ min}^{-1}$, the O/C ratio was close to ~ 4 , and the effluent of the reactor was composed of mainly CO_2 and H_2O , revealing that the dominating reaction was full oxidation of the methane. At a higher methane feed rate of $31.6 \text{ cm}^3 \text{ min}^{-1}$, the O/C ratio decreased to 1.08, and the effluent was composed of mainly H_2 and CO , revealing that the dominating reaction was POM.

Fig. 5 shows the POM performance of the hollow fiber membrane reactor at 950°C . It can be seen that after a short activation period of ~ 2 h involving the in-situ reduction of Ru catalyst, the reactor attained a desired stable state. Methane throughput conversion over 90% was obtained at a high methane feed rate of $31.6 \text{ cm}^3 \text{ min}^{-1}$ equivalent to $14.7 \text{ cm}^3 \text{ CH}_4 \text{ min}^{-1} \text{ cm}^{-2}$ membrane surface (at the lumen side) and oxygen permeation rate of $7.9 \text{ cm}^3 \text{ min}^{-1} \text{ cm}^{-2}$. The residence time for the reactor was estimated to be less than 0.03 s, indicating the fast POM reaction kinetics with the hollow fiber membrane reactor. On average, the effluent gas of the reactor was composed of 53.5% of H_2 , 35.7% of CO , 0.1% of CO_2 , 7.1% of H_2O and 3.6% of CH_4 . After 100 h of operation, a noticeable decrease of H_2 concentration and increase of H_2O concentration occurred, the cause for which is not clear at this

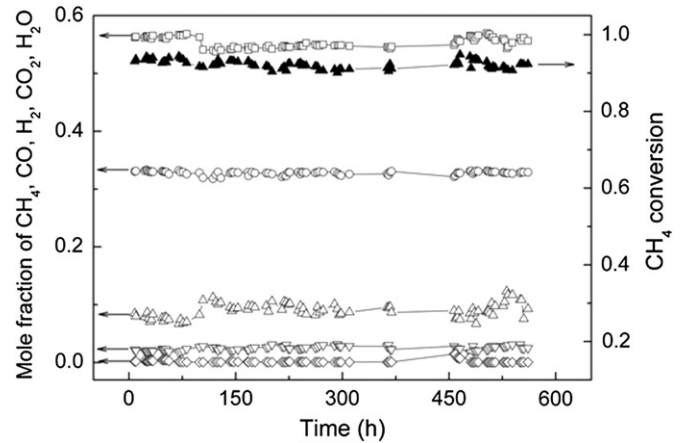


Fig. 5. POM performance of the hollow fiber membrane reactor. (■) H_2 mole fraction, (○) CO mole fraction, (Δ) H_2O mole fraction, (▽) CH_4 mole fraction, (◊) CO_2 mole fraction, (▲) methane conversion. Conditions: temperature = 950°C , methane feed rate = $31.6 \text{ cm}^3 \text{ min}^{-1}$.

moment. The test was voluntarily terminated after ~ 600 h of operation.

Fig. 6 shows the performance of a disk-shaped SOFC cell. The fuel cell was tested at a fixed temperature of 750°C and current density of 200 mA cm^{-2} . It exhibited a stable performance when running on the fuel (mainly H_2 and CO) converted from the methane by the membrane reactor. But, it failed shortly when methane was directly fed into the cell, which is attributed to the carbon deposition on the Ni-based anode.

4. Discussion

This study shows that the hollow fiber membrane reactor can reform methane at a high efficiency owing to the integration of separation of oxygen from air and POM reaction in a single space. The high oxygen permeation rate is attributed to the unique two-layer asymmetric structure of the YSZ–LSCF hollow fiber membrane and the large oxygen gradient imposed across the membrane along the radial direction [28]. The fast POM reaction kinetics is attributed to the high aspect ratio (length/diameter) of

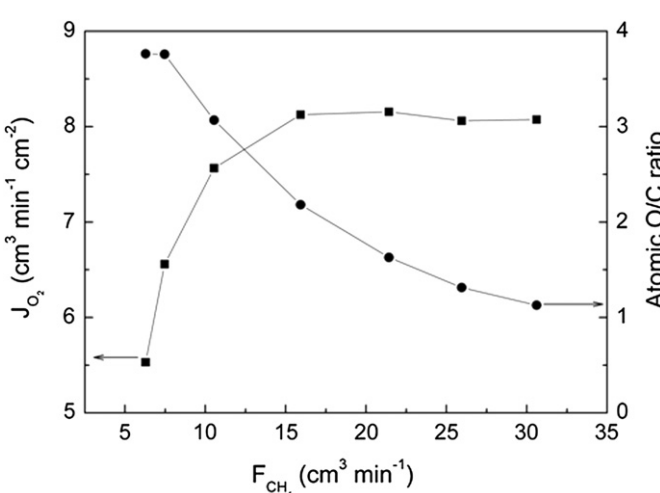


Fig. 4. Oxygen permeation rate (■) and atomic O/C ratio (●) as a function of methane feed rate at a fixed temperature of 950°C .

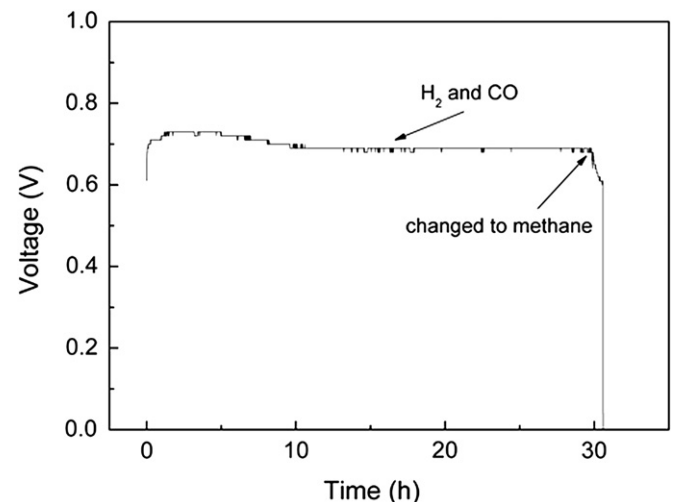


Fig. 6. Output voltage vs time for an SOFC operated at 750°C and current density of 200 mA cm^{-2} .

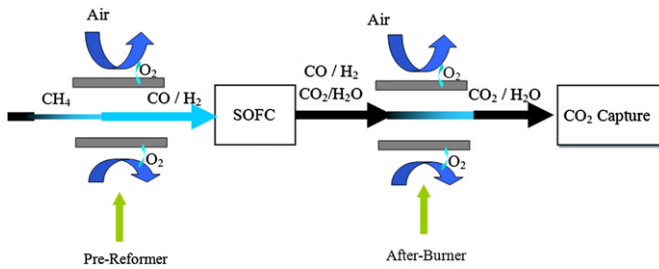


Fig. 7. Schematic of a methane-fuelled SOFC system with CO₂ capture.

the hollow fiber which allows sufficient collision of the methane molecules with the membrane surface (at the lumen side) where reaction of methane with the permeated oxygen occurs.

The fuel produced from methane by the hollow fiber membrane reactor had a desired composition. It has been shown that when the atomic O/C ratio is greater than 1 at 900 °C, and 0.82 at 700 °C, no carbon will deposit on the Ni-anode surface [11,12]. The fuel produced by the membrane reactor had a higher O/C ratio than those values, thus carbon will not deposit on the Ni-anode, giving rise to a stable performance of the SOFC. Moreover, the fuel did not contain nitrogen due to the use of the oxygen separation membrane and hence is rich in H₂ and CO. This is not only essential for achieving high energy efficiency of the fuel cell, but also crucial for efficient capture of CO₂ discharged from the fuel cell. A methane-fuelled SOFC system with CO₂ capture can be constructed by placing a membrane-based burner after the fuel cell (Fig. 7). Such a fuel cell system discharges only CO₂ and steam which can be separated easily through condensation of the steam by cooling.

As stated earlier, SR is highly endothermic reaction, thus a large quantity of heat needs to be fed into the reactor. In contrast, the POM reaction is mild exothermal, thus it is possible for the membrane reactor to be thermally self-sustained. The hollow fiber membrane has a high surface/volume ratio, thus it is possible to pack a large quantity of hollow fibers in a module [29]. Those two features combined may allow us to construct and operate a compact autothermal methane reformer for SOFC applications.

5. Conclusions

This work has shown that methane can be converted to H₂ and CO at a remarkably fast rate by a YSZ–LSCF hollow fiber membrane reactor through integration of POM and separation of oxygen from air in a single space. An SOFC can run on the fuel converted from methane by the membrane reactor. The mild exothermal nature of the POM reaction and high surface/volume ratio of the hollow fiber

membrane combined makes it possible to construct and operate a compact autothermal methane reformer for SOFC applications.

Acknowledgements

This work was partly supported National Science Foundation of China (Grant Nos.: 21076205, 50972138).

References

- [1] A. Weber, B. Sauer, A.C. Müller, D. Herbstritt, E. Ivers-Tiffée, Solid State Ionics 152–153 (2002) 543–550.
- [2] Y.H. Huang, R.I. Dass, Z.L. Xing, J.B. Goodenough, Science 312 (2006) 254–257.
- [3] B.C.H. Steele, I. Kelly, H. Middleton, R. Rudkin, Solid State Ionics 28–30 (Part 2) (1988) 1547–1552.
- [4] J.H. Koh, Y.S. Yoo, J.W. Park, H.C. Lim, Solid State Ionics 149 (2002) 157–166.
- [5] T. Kim, G. Liu, M. Boaro, J.M. Voohs, R.J. Gorte, O.H. Al-Madhi, B.O. Dabbousi, Journal of Power Sources 155 (2006) 231–238.
- [6] S. McIntosh, R.J. Gorte, Chemical Reviews 104 (2004) 4845–4865.
- [7] Z.L. Zhan, S.A. Barnett, Science 308 (2005) 844–847.
- [8] P. Vernoux, M. Guillodo, J. Fouletier, A. Hammou, Solid State Ionics 135 (2000) 425–431.
- [9] E.P. Murray, T. Tsai, S.A. Barnett, Nature 400 (1999) 649–651.
- [10] S.W. Tao, J.T.S. Irvine, Nature Materials 2 (2003) 320–323.
- [11] J.-H. Koh, B.-S. Kang, H.C. Lim, Y.-S. Yoo, Electrochemical and Solid-State Letters 4 (2001) A12–A15.
- [12] J.P. Tremblay, R.S. Gemmen, D.J. Bayless, Journal of Power Sources 171 (2007) 818–825.
- [13] E. Achenbach, E. Riemsche, Journal of Power Sources 52 (1994) 283–288.
- [14] A.L. Dicks, K.D. Pointon, A. Siddle, Journal of Power Sources 86 (2000) 523–530.
- [15] N. Laosiripojana, S. Assabumrungrat, Journal of Power Sources 163 (2007) 943–951.
- [16] S. Hosseini, S.M. Jafarian, G. Karimi, International Journal of Energy Research 35 (2011) 259–270.
- [17] P. Aguiar, D. Chadwick, L. Kershenbaum, Chemical Engineering Science 57 (2003) 1665–1677.
- [18] P.-W. Li, M.K. Chyu, Journal of Power Sources 124 (2003) 487–498.
- [19] D.J. Wilhelm, D.R. Simbeck, A.D. Karp, R.L. Dickenson, Fuel Processing Technology 71 (2001) 139–148.
- [20] A.C. Vosloo, Fuel Processing Technology 71 (2001) 149–155.
- [21] J.R. Rostrup-Nielsen, Catalysis Today 71 (2002) 243–247.
- [22] W.Q. Jin, S.G. Li, P. Huang, N.P. Xu, J. Shi, Y.S. Lin, Journal of Membrane Science 166 (2000) 13–22.
- [23] Z.P. Shao, W.S. Yang, Y. Cong, H. Dong, J.H. Tong, G.X. Xiong, Journal of Membrane Science 172 (2000) 177–188.
- [24] C.S. Chen, S.J. Feng, S. Ran, D.C. Zhu, W. Liu, H.J.M. Bouwmeester, Angewandte Chemie International Edition 42 (2003) 5196–5198.
- [25] H.H. Wang, A. Feldhoff, J. Caro, T. Schiestel, S. Werth, AIChE Journal 55 (2009) 2657–2664.
- [26] M.C. Zhan, W.D. Wang, T.F. Tian, C.S. Chen, Energy Fuels 24 (2010) 764–771.
- [27] T.F. Tian, W.D. Wang, M.C. Zhan, C.S. Chen, Catalysis Communications 11 (2010) 624–628.
- [28] J.J. Liu, T. Liu, W.D. Wang, J.F. Gao, C.S. Chen, Journal of Membrane Science 389 (2012) 435–440.
- [29] W. Li, J.J. Liu, C.S. Chen, Journal of Membrane Science 340 (2009) 266–271.
- [30] S.Q. Zhang, L. Bi, L. Zhang, W. Liu, International Journal of Hydrogen Energy 34 (2009) 7789–7794.